Published in final edited form as:
J Neurochem. 2014 July ; 130(1): 145–159. doi:10.1111/jnc.12700.

Alterations in Striatal-Enriched Protein Tyrosine Phosphatase (STEP) Expression, Activation and Downstream Signaling in Early and Late Stages of the YAC128 Huntington's Disease Mouse Model

Clare M. Gladding[1], **Jing Fan**[1], **Lily Y. J. Zhang**[1], **Liang Wang**[1], **Jian Xu**[2], **Edward H. Y. Li**[1], **Paul J. Lombroso**[2], and **Lynn A. Raymond**[1]

[1]Department of Psychiatry, Division of Neuroscience, Brain Research Centre, University of British Columbia, Vancouver, British Columbia, V6T 1Z3, Canada

[2]Child Study Center, Yale University School of Medicine, New Haven, Connecticut, 06520, U.S.A

Abstract

Striatal neurodegeneration and synaptic dysfunction in Huntington's disease (HD) are mediated by the mutant huntingtin protein (mHtt). MHtt disrupts calcium homeostasis and facilitates excitotoxicity, in part by altering NMDA receptor (NMDAR) trafficking and function. Presymptomatic (excitotoxin-sensitive) transgenic mice expressing full-length human mHtt with 128 polyglutamine repeats (YAC128 HD mice) show increased calpain activity and extrasynaptic NMDAR (Ex-NMDAR) localization and signaling. Furthermore, Ex-NMDAR stimulation facilitates excitotoxicity in wild-type cortical neurons via calpain-mediated cleavage of STriatal-Enriched protein tyrosine Phosphatase 61 (STEP61). The cleavage product, STEP33, cannot dephosphorylate p38 MAPK, thereby augmenting apoptotic signaling. Here, we show elevated extrasynaptic calpain-mediated cleavage of STEP61 and p38 phosphorylation, as well as STEP61 inactivation and reduced ERK1/2 phosphorylation in the striatum of 6-week old, excitotoxin-sensitive YAC128 mice. Calpain inhibition reduced basal and NMDA-induced STEP61 cleavage. However, basal p38 phosphorylation was normalized by a peptide disrupting NMDAR-PSD-95 binding but not by calpain inhibition. In 1-year old excitotoxin-resistant YAC128 mice, STEP33 levels were not elevated, but STEP61 inactivation and p38 and ERK1/2 phosphorylation levels were increased. These results show that in YAC128 striatal tissue, enhanced NMDAR-PSD-95 interactions contributes to elevated p38 signaling in early, excitotoxin-sensitive stages, and suggest that STEP61 inactivation enhances MAPK signaling at late, excitotoxin-resistant stages.

Keywords

Calpain; STEP; NMDA receptor; Extrasynaptic; Huntington's disease; p38 MAPK signaling

Correspondence: Lynn A. Raymond, MD, PhD, Department of Psychiatry, University of British Columbia, 4N3-2255 Wesbrook Mall, Vancouver, BC V6T 1Z3, lynn.raymond@ubc.ca, Phone: 604-822-0723, Fax: 604-822-7981.

The authors have no conflict of interest to declare.

Introduction

Huntington's disease (HD) is a neurodegenerative disorder caused by a polyglutamine repeat expansion in the huntingtin (Htt) protein, producing the pathological mutant huntingtin (mHtt) (HDCRG 1993). Synaptic dysfunction and striatal neurodegeneration in HD are attributed, in part, to abnormal localization, function and signaling of NMDA receptors (NMDARs) and subsequent elevated excitotoxicity (Arundine & Tymianski 2003, Graham *et al.* 2009, Lau & Zukin 2007, Shehadeh *et al.* 2006, Zeron *et al.* 2002). In presymptomatic yeast artificial chromosome mice expressing full-length Htt with 128 polyglutamine repeats (YAC128 HD mice), NMDARs traffic faster to the cell surface and accumulate at extrasynaptic sites (Fan *et al.* 2007, Gladding *et al.* 2012, Milnerwood *et al.* 2010). The NMDAR GluN2B subunit mediates increased vulnerability to excitotoxicity in mHtt-expressing striatal medium-spiny projection neurons (SPNs) (Fan *et al.* 2012, Gladding *et al.* 2012, Li *et al.* 2004, Milnerwood *et al.* 2010). Results of these studies are consistent with the hypothesis that Ex-NMDAR stimulation preferentially activates apoptotic signaling cascades (Hardingham *et al.* 2002, Leveille *et al.* 2008).

In presymptomatic YAC128 mice, mHtt-mediated disruptions in calcium homeostasis lead to enhanced activation of the calcium-dependent protease, calpain and membrane-bound synaptic, but not extrasynaptic, STriatal-Enriched protein tyrosine Phosphatase 61 (STEP61) (Cowan *et al.* 2008, Gafni & Ellerby 2002, Gladding *et al.* 2012, Kim *et al.* 2001). STEP61 dephosphorylates both the pro-survival MAPK, extracellular signal-regulated protein kinase 1/2 (ERK1/2), and the pro-apoptotic signaling molecule, p38 mitogen-activated protein kinase (p38 MAPK). Moreover, STEP61 dephosphorylates the GluN2B subunit, and increased STEP61 activation in the postsynaptic density (PSD) facilitates elevated Ex-NMDAR localization in the YAC128 striatum (Gladding *et al.* 2012). Notably, in wild-type (WT) cortical neurons, Ex-NMDAR stimulation triggers calpain-mediated cleavage of STEP61 to produce an inactive isoform, STEP33 (Xu *et al.* 2009); since STEP33 cannot bind or dephosphorylate its substrates, such as p38 MAPK, this contributes to increased apoptotic signaling. Preventing calpain-mediated cleavage of STEP61 is neuroprotective against both glutamate-induced neurotoxicity and oxygen and glucose deprivation (OGD) in WT cultures and cortical-striatal slices (Xu *et al.* 2009).

Increased p38 MAPK signaling has been observed in the striatum of young excitotoxin-sensitive YAC128 mice (Fan *et al.* 2012) and at later stages in the excitotoxin-resistant R6/1 HD mouse model (Saavedra *et al.* 2011). Increased extrasynaptic expression and binding of the GluN2B subunit to the scaffolding protein, postsynaptic density protein-95 (PSD-95) facilitates enhanced NMDA-induced p38 MAPK activation in the presymptomatic YAC128 striatum; this increase in GluN2B-PSD-95 coupling and p38 MAPK activation contributes to elevated striatal neuronal vulnerability to NMDA-induced apoptosis (Fan *et al.* 2012). By contrast, decreased STEP activity, resulting from phosphorylation and reduced expression rather than calpain cleavage, is linked to reduced vulnerability to excitotoxicity and increased phosphorylation and activation of both p38 MAPK and ERK1/2 in excitotoxin-resistant R6/1 mouse striatum (Saavedra *et al.* 2011).

It is not known whether calpain-mediated cleavage or phosphorylation-induced inactivation of extrasynaptic STEP61 alters the balance of striatal cell death/survival signaling in an excitotoxin-sensitive HD mouse model. Here, we used the YAC128 model at two different stages of disease: 6-week old presymptomatic mice, that show enhanced neuronal death in response to intrastriatal quinolinate (QUIN), an NMDAR agonist ("excitotoxin-sensitive"); and symptomatic 1-year old mice, that show resistance to intrastriatal QUIN-induced neurodegeneration, similar to other late-stage HD mouse models ("excitotoxin-resistant") (Graham *et al.* 2009, Saavedra *et al.* 2011). We investigated whether calpain-mediated cleavage of STEP61 contributes to altered p38 MAPK and/or ERK1/2 activation in the striatum from 6-week old YAC128 mice. We also determined whether alterations in STEP cleavage, expression or phosphorylation levels correlate with changes in p38 MAPK and ERK1/2 activation in 1-year old YAC128 mice. Results from this study broaden our understanding of mechanisms leading to excitotoxicity susceptibility and resistance in early and late stages of HD, respectively.

Materials and Methods

Transgenic mice

WT and YAC128 (line 55) mice bred on the FVB/N mouse strain were housed, cared and used according to the Canadian Council on Animal Care regulations at the University of British Columbia (UBC) Faculty of Medicine Animal Resource Unit (protocol # A11-0012). Either 6-week or 1-year old male mice were used for experiments. The ARRIVE guidelines were followed.

Peptides

The TAT-myc and TAT-STEP peptides were synthesized by the Keck Facility (Yale University). The TAT-myc peptide (containing the myelocytomatosis virus (myc) tag) served as the control. The TAT-STEP peptide spans the cleavage site such that calpain-mediated cleavage of STEP61 is prevented (Xu *et al.* 2009). Both peptides were cell permeable because of the human immunodeficiency virus-type 1 (HIV-1) transduction TAT domain. 2mM TAT-myc and 1mM TAT-STEP stock solutions were made in PBS (pH 7.4), aliquoted, stored at −80°C and thawed only once before use. For slice treatments, peptide stock solutions were diluted in artificial cerebrospinal fluid (aCSF, containing in mM): 125 NaCl, 2.5 KCl, 25 $NaHCO_3$, 1.25 NaH_2PO_4, 1 $MgCl_2$, 2 $CaCl_2$, 10 glucose, pH7.3–7.4, 300–310 mosmol L^{-1}) and sonicated briefly until completely dissolved.

The TAT-GluN2B9c and TAT-GluN2BAA peptides were purchased (AnaSpec and Peptides 2.0). The TAT-GluN2B9c peptide prevents PSD-95 binding to the GluN2B subunit C-terminus (Aarts *et al.* 2002). The TAT-GluN2BAA peptide was similar to TAT-GluN2B9c but had a double point mutation in the C-terminal tSXV motif such that it could not bind PSD-95. Both peptides were solubilized in sterile Milli-Q water as 1mM stocks and aliquots stored at −80°C until use.

Striatal dissections and brain slice preparation

To minimize pain, WT and YAC128 mice were halothane-anesthetized and decapitated. For whole-cell lysate preparations, striatum was dissected from whole brain in cold PBS on ice. To determine basal protein levels using subcellular fractionation, brains were rapidly removed and placed in ice-cold sucrose buffer (0.32M sucrose, 10mM HEPES, pH 7.4) containing protease and phosphatase inhibitor cocktails, as described (Gladding *et al.* 2012). For parasagittal slice preparation, brains were immersed in oxygenated (95% O_2-5% CO_2), chilled cutting aCSF containing a 3:1 Mg^{2+}: Ca^{2+} ratio to minimize NMDAR activation. 300μm parasagittal slices cut using a vibratome (Leica VT1000) were placed into continuously oxygenated normal aCSF (1:2 Mg^{2+}: Ca^{2+} ratio) to rest (1h, room temperature (RT)).

Parasagittal slice treatment

All slice treatments were performed using continuously oxygenated normal aCSF at RT. For calpain inhibition, slices were incubated in aCSF containing either DMSO (vehicle control) or calpeptin (Calbiochem; 15μM, 2h). For treatments with NMDA and calpeptin, slices were incubated in aCSF with DMSO (vehicle condition) or calpeptin (15μM, 1h) and subsequently placed in aCSF containing DMSO or NMDA (30μM, 70min) with or without calpeptin (15μM, 70min). To specifically inhibit calpain-mediated cleavage of STEP61, slices were incubated in aCSF containing either PBS (vehicle condition), or TAT-myc or TAT-STEP peptide (2μM, 1h). Slices were subsequently incubated in aCSF containing NMDA (30μM, 70min) with or without the TAT-myc and TAT-STEP peptides. This concentration of the TAT-STEP peptide has previously been shown to significantly reduce STEP33 production (Xu *et al.* 2009). For treatment with TAT-GluN2B9c or TAT-GluN2BAA peptides, slices were incubated in aCSF containing 200nM of either peptide (1h). This TAT-GluN2 9c concentration has been shown to significantly reduce the GluN2B-PSD-95 interaction (Fan *et al.* 2012). Slices were washed briefly in aCSF prior to harvesting tissue.

Whole-cell lysate preparations

To determine STEP expression and phosphorylation levels, as well as p38 and ERK1/2 phosphorylation in 6-week and 1-year old striata, whole-cell lysates were prepared using a protocol similar to that described previously (Saavedra *et al.* 2011). The striatum was homogenized in lysis buffer (1% Triton X-100, 50mM Tris-HCl, 10mM EGTA, 150mM NaCl, pH 7.5) containing ‘complete’ protease and ‘phosSTOP’ phosphatase inhibitor cocktails (Roche diagnostics). Samples were subsequently centrifuged at 16,000g (20min, 4°C) and the supernatant stored at −80°C until use. This preparation contains solubilized cytosolic and membrane proteins but should exclude the postsynaptic density (PSD) fraction.

After treating slices with either TAT-myc, TAT-STEP, TAT-GluN2B9c or TAT-GluN2BAA peptides, whole-cell lysates were obtained using a protocol described previously (Fan *et al.* 2012). After treatment, slices were placed in ice-cold PBS with 5mM EDTA and 5mM EGTA and the striatal tissue dissected on ice. The tissue was subsequently homogenized in 1% NP40-containing lysis buffer (50mM Tris, 150mM NaCl, pH 7.4)

containing ‘complete’ protease and ‘phosSTOP’ phosphatase inhibitor cocktails (Roche diagnostics). Striatal homogenates were solubilized using ultrasonication for 10s and rotated to lyse samples (> 2h, 4°C).

Subcellular fractionation

To obtain PSD, non-PSD and S2 (cytosolic) fractions, a subcellular fractionation protocol was followed as described previously (Milnerwood *et al.* 2010). It is possible to isolate PSD and non-PSD fractions on the basis that the PSD is Triton X-100 insoluble whereas the non-PSD is soluble (Goebel-Goody *et al.* 2009, Milnerwood *et al.* 2010, Pacchioni *et al.* 2009). All buffers contained protease and phosphatase inhibitor cocktails in addition to 40mM β-glycerophosphate, 20mM sodium pyrophosphate, 1mM sodium orthovanadate, 30mM NaF, 1mM EDTA, 1mM EGTA. For calpain inhibition experiments, 15μM calpeptin was also included. Fractions were stored at −80°C until use.

Western blotting

Western blotting was performed as described previously (Gladding *et al.* 2012, Milnerwood *et al.* 2010). In brief, sample protein concentration was normalized, separated via 10% sodium dodecyl sulphate-polyacrylamide gel electrophoresis (SDS-PAGE) and transferred to polyvinylidene difluoride (PVDF) membrane. After transfer, membranes were blocked in 3% BSA or 5% milk in 0.5% Tween-20 in TBS (TBST) (1h, RT), and incubated with primary antibodies (3% BSA in TBST, overnight, 4°C). After washing, blots were incubated with horseradish peroxidase (HRP)-coupled secondary antibodies (3% BSA or 5% milk in TBST, 2h, RT), washed and visualized using enhanced chemiluminescence substrate (ECL, Amersham) and exposure to film (Amersham). In some cases, β-actin, tubulin and phosphorylated p38 MAPK were visualized using alkaline phosphatase (AP)-conjugated secondary antibodies and a Lumi-phos WB chemiluminescent substrate detection system (Pierce).

Primary antibodies used were rabbit N-terminal anti-GluN2B (AGC-003, Alomone, 1:500), goat anti-β-actin (sc-1616, Santa Cruz, 1:1500), mouse anti-synaptophysin (S5768, Sigma, 1:1000), mouse anti-PSD-95 (MA1-045, Affinity BioReagents, 1:500), mouse anti-STEP (23E5; sc-23892, Santa Cruz, 1:500), rabbit anti-phosphorylated STEP (pSTEP61 and pSTEP46; AB2208, Millipore, 1:200), mouse anti-p38 α/β (sc-7972, Santa Cruz, 1:200), rabbit anti-phosphorylatedp38 (Thr180/Tyr182; 4511, Cell Signaling, 1:200), mouse anti-ERK1/2 (4696, Cell Signaling, 1:1000; both 42 and 44 kDa bands quantified), rabbit anti-phosphorylated ERK1/2 (4370, Cell Signaling, 1:500; both 42 and 44 kDa bands quantified), and goat anti-tubulin (sc-9935, Santa Cruz, 1:750). Secondary antibodies used were anti-mouse HRP-conjugated (NA931V, Amersham, 1:5000–1:10,000), anti-rabbit HRP-conjugated (NA934V, Amersham, 1:5000–1:10,000), anti-rabbit AP-conjugated (S3738, Promega, 1:6000), anti-goat AP-conjugated (sc-2037, Santa Cruz, 1:5000).

Data analysis and statistics

Image J (NIH) was used to quantify the optical density of immunoreactive bands for western blot analysis. Band densities were normalized to the protein loading controls β-actin (subcellular fractions) or tubulin (whole cell lysates). Statistical analysis was performed

using GraphPad Prism and Microsoft Excel programs. Data are presented as the mean +/− SEM. Significant differences were determined using two-tailed paired and unpaired *t*-tests, one sample *t*-tests, two-way ANOVAs and Bonferroni's *post hoc* tests as indicated; p values < 0.05 were deemed significant.

Results

Increased calpain-mediated cleavage and phosphorylation-induced inactivation of STEP61 correlate with elevated p38 MAPK signaling in excitotoxin-sensitive YAC128 striatum

STEP61 can be inactivated by calpain-mediated cleavage to produce the inactive isoform STEP33, or by protein kinase A (PKA)-mediated phosphorylation (Paul *et al.* 2000). In the excitotoxin-sensitive striatum of presymptomatic (1–2 month old) YAC128 mice, Ex-NMDAR activity and p38 MAPK phosphorylation are enhanced (Fan *et al.* 2012, Milnerwood *et al.* 2010). Previous work showed these processes can be linked in rat cortical neurons via calpain-mediated cleavage of STEP61 (Xu *et al.* 2009). STEP46 is another isoform found mainly in the cytosol (Braithwaite *et al.* 2006, Braithwaite *et al.* 2008), where it is less responsive to NMDAR activity. However, it is yet to be investigated whether altered STEP61/STEP46 activity and/or expression mediate changes in p38 and ERK1/2 activation in the excitotoxin-sensitive stage of an HD mouse model. We therefore examined striatal tissue wholecell lysates from 6-week old YAC128 mice. STEP61, STEP46 and STEP33 isoforms, as well as phosphorylated STEP61 (pSTEP61) and STEP46 (pSTEP46), were quantified relative to the protein loading control, tubulin (Fig. 1A–C). There was significantly decreased STEP61 expression and increased STEP33 production compared to WT mice (Fig. 1B), but no difference in STEP46 levels between WT and YAC128 mice. These findings suggest that STEP61 is cleaved by calpain at the excitotoxin-sensitive stage of the disease in YAC128 mice.

Upon NMDAR-mediated calcium influx, activation of the calcium-dependent phosphatase calcineurin dephosphorylates STEP61 at its kinase domain serine 221 residue (Paul *et al.* 2003), thus allowing association with substrates such as p38 MAPK and ERK and their subsequent dephosphorylation. Although, there was no significant difference in pSTEP46 levels, pSTEP61 levels were significantly higher in the YAC128 striatum compared to WT mice (Fig. 1C), indicating more inactive STEP61 at this age. Phosphorylation levels of STEP substrates were significantly reduced for ERK1/2 but significantly increased for p38 MAPK in excitotoxin-sensitive YAC128 striatum compared to WT mice (Fig. 1D, E). Because the PSD is largely insoluble in 1% Triton X-100, the whole-cell lysate preparation contained mainly cytosolic and extrasynaptic membrane proteins. Together, these results suggest that increased calpain-mediated cleavage, and/or elevated inactivation of extrasynaptic STEP61 may contribute to increased p38 MAPK apoptotic signaling in 6-week old YAC128 mice. In contrast, decreased ERK1/2 phosphorylation does not correlate with reduced expression and activity of extrasynaptic STEP61.

Increased inactivation of STEP61 correlates with elevated ERK and p38 MAPK signaling in excitotoxin-resistant YAC128 striatum

At later stages in the excitotoxin-resistant R6/1 HD mouse model, elevated ERK and p38 MAPK signaling occurs as a result of inactivation by phosphorylation rather than by calpain-mediated cleavage of STEP61 (Saavedra *et al.* 2011). After 10-months of age, YAC128 mice become resistant to QUIN-induced striatal neurotoxicity and show reduced NMDAR-mediated membrane currents (Graham *et al.* 2009). To determine whether STEP expression or activity is altered at later ages in the YAC128 striatum, whole-cell striatal lysates were isolated from 1-year old WT and YAC128 mice and probed for STEP and pSTEP levels, as well as ERK1/2 and p38 MAPK activation (Fig. 2A, D). Quantification indicates no difference in STEP46 and STEP33 levels, but a significant decrease in YAC128 STEP61 levels compared to WT mice (Fig. 2B). Furthermore, YAC128 mice displayed a significant increase in pSTEP61 levels but no difference in pSTEP46 levels relative to WT mice (Fig. 2C). There was a significant increase in both pERK/ERK and p-p38/p38 ratios in the YAC128 striatum compared to WT mice (Fig. 2D, E). These results suggest that STEP61 inactivation by phosphorylation rather than by calpain-mediated cleavage contributes to altered cell survival/death signaling in the 1-year old excitotoxin-resistant YAC128 striatum.

Enhanced calpain-mediated cleavage of STEP61 at extrasynaptic sites in excitotoxin-sensitive YAC128 striatum

Previous studies have shown that calpain activation and GluN2B-containing NMDAR expression are both increased extrasynaptically in presymptomatic YAC128 mice (Gladding *et al.* 2012, Milnerwood *et al.* 2010). To determine whether enhanced Ex-NMDAR localization and signaling is associated with extrasynaptic calpain-mediated cleavage of STEP61 at this stage, we isolated synaptic (PSD), extrasynaptic-enriched (non-PSD), and cytosolic (S2) fractions from the striatal tissue of 6-week old WT and YAC128 mice. The accuracy of the subcellular fractionation procedure was confirmed by western blots demonstrating enrichment of PSD-95 or synaptophysin in the PSD versus non-PSD fraction, respectively, as previously described (data not shown) (Milnerwood *et al.* 2010). PSD, non-PSD and S2 fractions were probed using the STEP antibody that recognises STEP61 and STEP46 isoforms and the calpain cleavage product, STEP33 (Fig. 3A). STEP61 was specifically enriched at extrasynaptic sites in striatal tissue from both WT and YAC128 mice as previously observed in the striatum, hippocampus and cortex (Gladding *et al.* 2012, Goebel-Goody *et al.* 2009, Jiang *et al.* 2011). As expected, the STEP46 isoform and calpain cleavage product STEP33 were enriched in the cytosol and weak or absent in PSD and non-PSD fractions (Fig. 3A). We found a significant decrease in STEP61 in the non-PSD fraction in YAC128 compared to WT striatum, and a concomitant increase in the cytosolic STEP33 cleavage product (Fig. 3A, B). There was no reduction in synaptic STEP61 levels (Fig. 3A, B), suggesting that calpain-mediated cleavage of STEP61 is specifically enhanced in the extrasynaptic membrane compartment of the presymptomatic YAC128 striatum. Furthermore, there was no change in expression of STEP46 in the non-PSD, PSD or S2 fractions, indicating that the STEP61 isoform rather than STEP46 is targeted specifically by calpain for cleavage (Fig. 3A, B).

We next determined the effect of calpain inhibition on STEP levels by incubating 6-week old WT and YAC128 parasagittal cortical-striatal slices with the calpain inhibitor, calpeptin before dissecting out the striatum for subcellular fractionation. As observed after whole striatum fractionations, YAC128 cytosolic STEP33 levels were significantly increased compared to WT in the vehicle (DMSO-treated) condition (Fig. 3C and D). Calpeptin treatment significantly reduced STEP33 in YAC128 to WT levels (Fig. 3D). Extrasynaptic STEP61 levels in the non-PSD fraction also increased after calpain inhibition in the YAC128 but not WT striatum (blots and quantification not shown; STEP61/β-actin ratios for DMSO: WT, 0.46 ± 0.08; YAC128, 0.44 ± 0.06; for calpeptin: WT, 0.66 ± 0.11; YAC128, 0.73 ± 0.12; two-way ANOVA, significant difference for treatment in YAC128 ($F_{1,10}$ = 12.17, $p < 0.01$); $p < 0.05$ by Bonferroni *post hoc* test; n = 6.). In contrast, calpain inhibition had no effect on STEP61 levels in the PSD fraction (blots and quantification not shown; STEP61/β-actin ratios for DMSO: WT, 0.56 ± 0.12; YAC128, 0.28 ± 0.03; for calpeptin: WT, 0.38 ± 0.08; YAC128, 0.31 ± 0.08; two-way ANOVA, $p > 0.05$, n = 5).

As previously reported (Gladding *et al.* 2012), calpain inhibition also significantly reduced cleaved GluN2B expression in the non-PSD but not PSD fraction of the presymptomatic YAC128 striatum (blots and quantification not shown; YAC128 cleaved GluN2B/β-actin ratios for non-PSD: DMSO, 0.84 ± 0.11; calpeptin, 0.47 ± 0.07; for PSD: DMSO, 0.70 ± 0.11; calpeptin, 0.78 ± 0.15; two-way ANOVA, significant difference for treatment in non-PSD ($F_{1,10}$ = 24.23, $p < 0.001$); $p < 0.01$ by Bonferroni *post hoc* test; n = 6). To confirm that vehicle alone had no effect on protein expression, experiments were also performed in which DMSO was not included throughout (blots not shown); however, calpeptin still had the same effect on STEP61, STEP33 and cleaved GluN2B levels relative to the untreated condition. Together, these results indicate that calpain activation is elevated at extrasynaptic sites in the 6-week old YAC128 striatum, resulting in cleavage of STEP61 to generate the inactive isoform, STEP33.

NMDA-induced calpain cleavage of STEP is blocked by calpeptin in presymptomatic YAC128 mice

WT cortical neurons that have been treated with glutamate or exposed to Ex-NMDAR stimulation display increased calpain-mediated cleavage of STEP61, which is blocked by calpeptin (Xu *et al.* 2009). We next determined whether Ex-NMDAR stimulation induces calpain-mediated cleavage of STEP61 in 6-week old YAC128 striatum, and whether this can be prevented by calpeptin. WT and YAC128 parasagittal cortical-striatal slices were treated with NMDA, with or without pre-treatment with calpeptin, followed by probing striatal cytosolic fractions for STEP and β-actin (Fig. 4A). In both WT and YAC128 mice, NMDA significantly increased striatal STEP33 production, which was reduced significantly by calpeptin treatment (Fig. 4B). However, when compared to the vehicle-only condition, calpeptin significantly attenuated NMDA-induced STEP33 production in the YAC128 but not WT striatum.

To determine whether calpeptin blocks extrasynaptic but not synaptic calpain activation, non-PSD and PSD samples were probed with an N-terminal GluN2B antibody that recognizes both full-length (180 kDa) and calpain-cleaved (115 kDa) GluN2B (Fig. 4C and

E). Compared to the NMDA treatment condition, calpeptin significantly reduced calpain-mediated cleavage of GluN2B in the YAC128 but not WT non-PSD fraction (Fig. 4D). However, there was no effect of calpeptin on synaptic cleaved GluN2B levels in either WT or YAC128 mice (Fig. 4F). These data suggest that Ex-NMDAR stimulation increases calpain-mediated cleavage of STEP61 and GluN2B at extrasynaptic sites. The finding that calpeptin has a larger effect in 6-week old YAC128 mice relative to WT implicates a greater disruption of calcium regulation at extrasynaptic sites at the excitotoxin-sensitive stage of the YAC128 mice.

Specific inhibition of NMDA-induced calpain cleavage of STEP61 in presymptomatic YAC128 striatum

A synthetic peptide spanning the STEP calpain cleavage site reduces STEP33 production and p38 MAPK activation after stimulating WT cortical neurons with glutamate (Xu *et al.* 2009). This TAT-STEP peptide was therefore used to block calpain-mediated cleavage of STEP61 in 6-week old YAC128 striatum after Ex-NMDAR stimulation. WT and YAC128 parasagittal cortical-striatal slices were incubated with NMDA with or without pre-treatment with the TAT-myc control peptide or the inhibitory TAT-STEP peptide. After probing whole-cell lysates for STEP and tubulin, we found significantly increased STEP33 production after NMDA treatment in YAC128 mice but not WT, relative to the control (Fig. 5A, B). A significant increase in YAC128 STEP33 levels was also observed with NMDA relative to the control in the presence of the TAT-myc, but not the TAT-STEP peptide. The data indicate that NMDA-induced calpain-mediated cleavage of STEP can be prevented by a synthetic inhibitory peptide in presymptomatic YAC128 striatal tissue.

Increased calpain-mediated cleavage of STEP61 does not elevate p38 MAPK activity in excitotoxin-sensitive YAC128 striatum

Presymptomatic YAC128 mice show elevated striatal p38 MAPK activity, which can be attenuated by the Ex-NMDAR antagonist, memantine (Dau *et al.* 2014). Although STEP inactivation is also elevated at this age, we hypothesized that elevated STEP61 cleavage contributes to increased basal p38 phosphorylation in 6-week old YAC128 mice. To test this hypothesis, WT and YAC128 parasagittal cortical-striatal slices were treated with either vehicle or calpeptin before probing cytosolic fractions for p-p38 and p38 MAPK. Calpeptin had no effect on p-p38/p38 ratios in either WT or YAC128 striatum (Fig. 6A; quantification not shown; calpeptin/DMSO p-p38/p38 ratios for WT, 1.17 ± 0.10; YAC128, 0.99 ± 0.06; one-sample *t*-test, $p > 0.05$, n = 5). Thus, we found no correlation between increased basal calpain-mediated cleavage of STEP61 and elevated p38 MAPK activation.

We also investigated the effect of specifically inhibiting calpain-mediated cleavage of STEP61 on NMDA-induced p38 activation. WT and YAC128 parasagittal cortical-striatal slices were incubated with NMDA with or without pre-treatment with the TAT-myc control peptide or the inhibitory TAT-STEP peptide. Although the TAT-STEP peptide prevented STEP61 cleavage (Fig. 5A, B), it did not significantly affect YAC128 p38 phosphorylation levels after NMDA treatment (blots and quantification not shown; p-p38/p38 ratios for WT: NMDA, 1.08 ± 0.49; NMDA plus TAT-STEP, 1.09 ± 0.47; NMDA plus TAT-myc, 0.91 ± 0.24; for YAC128: NMDA, 1.19 ± 0.18; NMDA plus TAT-STEP, 1.39 ± 0.26; NMDA plus

TAT-myc, 0.93 ± 0.19; one-sample *t*-test and a two-way ANOVA, $p > 0.05$, n = 4). Therefore, increased Ex-NMDAR-induced calpain cleavage of STEP61 is not correlated with elevated p38 MAPK activation in the excitotoxin-sensitive YAC128 striatum.

Elevated basal p38 activation is dependent upon GluN2B-PSD-95 interactions in presymptomatic YAC128 striatum

A previous study suggested that increased extrasynaptic expression and interactions of GluN2B and PSD-95 enhance p38 MAPK activation in the presymptomatic YAC128 striatum (Fan *et al.* 2012). A TAT-GluN2B9c peptide that specifically blocks GluN2B-PSD-95 interactions decreased NMDA-induced p38 MAPK activation in the YAC128 but not WT striatum. To test the hypothesis that increased basal p38 MAPK activation is attributed, in part, to elevated GluN2B-PSD-95 binding, 6-week old WT and YAC128 parasagittal cortical-striatal slices were incubated with either TAT-GluN2B9c or control TAT-GluN2BAA peptides. Consistent with a previous study (Fan *et al.* 2012) and current data (Fig. 1E), basal p38 MAPK activation was elevated in the YAC128 striatum relative to WT, in both untreated and TAT-GluN2BAA peptide conditions (Fig. 6B, C). However, the significant increase in YAC128 basal p38 MAPK activation was abolished after treatment with the TAT-GluN2B9c peptide. Together, these data demonstrate that increased GluN2B-PSD-95 interactions, but not elevated calpain-mediated cleavage of STEP61, contribute to enhanced basal p38 MAPK activation in the excitotoxin-sensitive YAC128 striatum.

Discussion

Synaptic dysfunction and excitotoxicity in HD are partly mediated by the deleterious effect of mHtt on NMDAR trafficking, localization and function (Gladding & Raymond 2011). Previously, we reported that increased activation of two calcium-dependent enzymes, calpain and STEP61, contributes to enhanced Ex-NMDAR expression in the striatum of presymptomatic YAC128 mice (Gladding *et al.* 2012); however, increased STEP61 activation occurred specifically in the PSD. The current study extends those results to demonstrate that STEP61 is cleaved by calpain at extrasynaptic sites and shows increased phosphorylation (inactivation) in striatal whole-cell lysates. Although Ex-NMDAR stimulation facilitates excitotoxicity and elevated p38 MAPK activation via calpain-mediated cleavage of STEP61 in WT cortical neurons (Xu *et al.* 2009), the current study indicates that increased GluN2B-PSD-95 interactions rather than calpain-mediated cleavage of STEP61 leads to increased p38 MAPK activation in excitotoxin-sensitive YAC128 striatum (Fan *et al.* 2012). We also show that striatal STEP61 inactivation in both 6-week old (presymptomatic) and 1-year old (symptomatic) YAC128 mice may contribute to elevated p38 activation in early and late HD, as well as to ERK1/2 activation in later, excitotoxin-resistant HD stages.

Elevated extrasynaptic calpain-mediated cleavage of STEP61 in excitotoxin-sensitive YAC128 mice

STEP61 is the main active isoform present at synaptic and extrasynaptic membranes and plays an important role in modulating the function/trafficking of substrates, including the GluN2B subunit, protein tyrosine kinase Fyn, p38 MAPK and ERK1/2 (Johnson &

Lombroso 2012). Calpain activation dramatically alters the function and localization of STEP61, directly impacting downstream apoptotic and cell survival signaling cascades. Upon an ischemic insult or direct Ex-NMDAR activation, calpain-mediated cleavage of STEP61 causes its redistribution from the plasma membrane to the cytosol, whilst also reducing its activity and resulting in net increased substrate phosphorylation, including p38 MAPK (Braithwaite *et al.* 2008, Xu *et al.* 2009). Enhanced p38 MAPK activation increases apoptotic signaling and excitotoxicity, consistent with the hypothesis that Ex-NMDAR stimulation activates cell death pathways (Hardingham *et al.* 2002, Leveille *et al.* 2008).

In the presymptomatic, excitotoxin-sensitive YAC128 striatum, we observed increased calpain-mediated cleavage of STEP61 in whole-cell lysates and extrasynaptic membranes, producing the inactive isoform, STEP33. The calpain inhibitor, calpeptin, reduced YAC128 STEP33 expression to WT levels, which correlated with increased extrasynaptic STEP61 expression. After stimulating extrasynaptic receptors with NMDA, calpeptin also significantly reduced the increase in STEP33 in both WT and YAC128 striata; however, when compared to the controls, there was a larger reduction in STEP33 expression in the YAC128 striatum. Also, calpeptin reduced YAC128 but not WT cleaved GluN2B levels in the extrasynaptic but not PSD fraction. Finally, the calpain cleavage inhibitory STEP peptide also reduced striatal NMDA-induced calpain cleavage of STEP61 in YAC128 but not WT striatum. These data support the hypothesis that Ex-NMDAR activation increases extrasynaptic calpain activation and cleavage of STEP, and that this signaling is likely to be enhanced in early disease pathogenesis.

Enhanced extrasynaptic calpain cleavage of STEP does not increase p38 MAPK activation in excitotoxin-sensitive YAC128 mice

Previous studies have reported that both calpain and p38 MAPK activation are enhanced in the YAC128 mouse striatum at 1–2 months (Cowan *et al.* 2008, Fan *et al.* 2012, Gladding *et al.* 2012). However, in the present study, there was no effect of either calpeptin or the STEP cleavage inhibitory peptide on YAC128 p38 MAPK phosphorylation levels, either basally or after NMDA treatment. Furthermore, at 4-months of age in the YAC128 striatum, calpain activation is similar to WT levels, whereas p38 MAPK phosphorylation levels remain high (Dau *et al.* 2014). These findings support the conclusion that calpain-mediated cleavage of STEP does not contribute to enhanced p38 MAPK activation in the excitotoxin-sensitive YAC128 striatum.

Calpain-mediated cleavage of STEP61 and p38 MAPK activation result after Ex-NMDAR stimulation in WT cortical neurons or after subjecting cortical-striatal slices to OGD treatment (Xu *et al.* 2009). Those data are in agreement with a report indicating that both GluN2B-containing NMDARs and p38 MAPK signaling cascade are enriched extrasynaptically in WT cortex (Jiang *et al.* 2011). In contrast, in our study calpain cleavage of STEP61 appears to be a consequence of enhanced Ex-NMDAR activity, but it is the elevated interactions between PSD-95 and GluN2B-containing Ex-NMDARs that increases pro-apoptotic p38 MAPK activation in presymptomatic HD striatum (Fan *et al.* 2012). Differences in results could be because the current study investigates an animal model of chronic, progressive neurodegeneration or because the mechanism observed is dependent

upon the brain area, *in vitro* system or the type or duration of NMDAR stimulation used. For example, sustained, but not transient, NMDAR activation triggers calpain-mediated cleavage of STEP61 and p38 MAPK activation in cortical-striatal co-cultures (Poddar *et al.* 2010). Here, the effects of calpeptin and the STEP cleavage inhibitory peptide on p38 MAPK activation were assessed at only one time point; further experiments are required to determine whether NMDA-induced increases in p38 MAPK phosphorylation are time-dependent.

If STEP61 cleavage is not involved in elevating p38 MAPK phosphorylation, what are the consequences of this cleavage in early HD? Reduced levels of STEP61 could be increasing the phosphorylation levels of other substrates such as Fyn or proline-rich tyrosine kinase 2 (Pyk2) in the striatum (Nguyen *et al.* 2002, Xu *et al.* 2012). Increased phosphorylation and activity of Fyn may facilitate increased forward trafficking of NMDARs to the cell surface in YAC128 SPNs (Dunah *et al.* 2004, Fan *et al.* 2007). Furthermore, in response to elevated calcium levels, phosphorylated active Pyk2 recruits the growth factor receptor-bound protein 2 (Grb2)/Sos adaptor complex which is coupled to MAPK signaling cascades such as ERK and c-Jun amino-terminal kinase (JNK) (Blaukat *et al.* 1999, Lev *et al.* 1995, Xu *et al.* 2012). Thus, increased STEP61 cleavage, enhancing Pyk2 activation, could contribute to elevated pro-apoptotic JNK signaling in HD (Fan *et al.* 2012, Liu *et al.* 2000). Further studies are required to determine other substrates that would be affected by enhanced calpain-mediated cleavage of STEP61 in presymptomatic HD mice.

Future work will also determine whether preventing calpain-mediated cleavage of STEP61 is neuroprotective in an excitotoxin-sensitive HD mouse model. It is possible that STEP61 cleavage augments apoptotic signaling cascades other than p38 MAPK and contributes to excitotoxicity in early HD. However, preventing calpain-mediated cleavage of STEP61 may not be sufficient to completely restore its normal functioning, since STEP61 inactivation via phosphorylation also occurs in presymptomatic HD mice. A combined approach would therefore be required to increase both STEP61 expression and activity levels at this early disease stage.

GluN2B-PSD-95 interactions contribute to increased p38 MAPK activation in the presymptomatic YAC128 striatum

Our finding that disrupting GluN2B-PSD-95 interactions decreases basally enhanced striatal p38 MAPK activation in 6-week old YAC128 mice is consistent with a previous report, indicating that GluN2B and PSD-95 show increased binding extrasynaptically (Fan *et al.* 2012). This may facilitate p38 MAPK activation by activating SynGAP and nNos signaling cascades in early HD stages (Aarts *et al.* 2002, Cao *et al.* 2005, Rumbaugh *et al.* 2006, Soriano *et al.* 2008). Furthermore, both p38 MAPK inhibition and the TAT-GluN2B9c peptide reduce NMDA-induced apoptosis in YAC128 striatal neurons to WT levels (Fan *et al.* 2009, Fan *et al.* 2012). Increased p38 MAPK activation stimulates downstream pro-apoptotic signaling cascades such as Bax translocation, cytochrome-c release, mitochondrial membrane permeabilization and caspase activation (Ghatan *et al.* 2000, Gomez-Lazaro *et al.* 2007) Therefore, Ex-NMDAR-mediated p38 MAPK signaling likely contributes to striatal neurodegeneration and neuronal dysfunction in early HD stages.

STEP inactivation occurs in both excitotoxin-resistant and sensitive HD stages

In this study, the expression and phosphorylation levels of STEP61 and two of its substrates, p38 MAPK and ERK1/2, were investigated in both presymptomatic (excitotoxin-sensitive) and symptomatic (excitotoxin-resistant) YAC128 mice. In the early stage of YAC128 disease progression, we have published that STEP61 is more active in the PSD (Gladding *et al.* 2012), consistent with data from this study demonstrating reduced phosphorylation of the pro-survival MAPK, ERK1/2. Here, we also found increased phosphorylation and inactivation of extrasynaptic STEP61, which correlates with elevated pro-apoptotic p38 MAPK signaling. So although we show evidence for a strong role of Ex-NMDAR-PSD-95 signaling in elevating p38 MAPK activity, extrasynaptic STEP inactivation could also contribute.

In 1-year old YAC128 mice, our findings suggest that STEP inactivation and decreased expression rather than calpain-mediated cleavage contribute to increased p38 MAPK signaling. MHtt expression may decrease STEP61 transcription and also facilitate dysregulation of the PKA pathway, leading to increased STEP61 phosphorylation (Saavedra *et al.* 2011). Inactivation of synaptic STEP61 at later, excitotoxin-resistant HD stages could also underlie the increase in neuroprotective ERK1/2 signaling. Our data obtained in 1-year old symptomatic YAC128 mice are consistent with results obtained in the excitotoxin-resistant R6/1 HD mouse model, in which increased p38 MAPK and ERK1/2 phosphorylation levels were partly attributed to decreased STEP61 expression and activity (Saavedra *et al.* 2011).

Conclusions

This study helps to elucidate the complex molecular mechanisms underlying changes in apoptotic and neuroprotective signaling in excitotoxin-sensitive and resistant stages of HD. It is important to understand the variation in disease progression in different HD mouse models in order to draw conclusions from mechanistic studies. Although increased Ex-NMDAR expression and signaling facilitate calpain-mediated cleavage of extrasynaptic STEP61, this does not contribute to increased p38 MAPK activation in the presymptomatic YAC128 striatum. Instead, STEP61 inactivation or signaling downstream of the GluN2B-PSD-95 complex may be more relevant in contributing to the early pathophysiology of HD. As the disease progresses in YAC128 mice, NMDAR currents and expression are dramatically reduced (Cowan *et al.* 2008, Graham *et al.* 2009), and it is likely that mHtt-mediated STEP61 inactivation and decreased expression facilitate increased ERK1/2 and p38 MAPK signaling (Saavedra *et al.* 2011). Although other mechanisms may also be at play, enhanced pro-survival ERK1/2 activity likely contributes to the switch to excitotoxin-resistance in 1-year old YAC128 mice. In understanding more about presymptomatic disease pathogenesis, these results will aid discovery and development of novel therapeutics for prevention or early treatment of HD.

Acknowledgments

This study was supported by the Canadian Institutes of Health Research (CIHR MOP-12699 to L.A.R.; a joint CIHR-Huntington Society of Canada postdoctoral fellowship to C.M.G.), the Cure Huntington Disease Initiative

(CHDI, to L.A.R.) and the National Institutes of Health (NIH MH091037 and MH52711 to P.J.L.). C.M.G. was also a Hereditary Disease Foundation (HDF) Scholar.

Abbreviations

aCSF	artificial cerebrospinal fluid
AP	alkaline phosphatase
ERK	extracellular signal-regulated protein kinase
Ex-NMDARs	extrasynaptic NMDARs
Grb2	growth factor receptor-bound protein 2
HD	Huntington's disease
HIV-1	human immunodeficiency virus-type 1
HRP	horseradish peroxidase
Htt	huntingtin
JNK	c-Jun amino-terminal kinase
KIM	kinase-interacting motif
MAPK	mitogen-activated protein kinase
mHtt	mutant huntingtin
myc	myelocytomatosis virus
NMDARs	NMDA receptors
OGD	oxygen and glucose deprivation
PKA	protein kinase A
PSD	postsynaptic density
PSD-95	postsynaptic density protein-95
PVDF	polyvinylidene difluoride
Pyk2	proline-rich tyrosine kinase 2
QUIN	quinolinate
SDS-PAGE	sodium dodecyl sulphate-polyacrylamide gel electrophoresis
RT	room temperature
SEM	standard error of the mean
SPN	striatal medium-spiny projection neuron
STEP	STriatal-Enriched protein tyrosine Phosphatase
TAT	trans-activating transduction
TBST	tris-buffered saline with 0.5 % tween-20
WT	wild-type

YAC yeast artificial chromosome

References

Aarts M, Liu Y, Liu L, Besshoh S, Arundine M, Gurd JW, Wang YT, Salter MW, Tymianski M. Treatment of ischemic brain damage by perturbing NMDA receptor- PSD-95 protein interactions. Science. 2002; 298:846–850. [PubMed: 12399596]

Arundine M, Tymianski M. Molecular mechanisms of calcium-dependent neurodegeneration in excitotoxicity. Cell Calcium. 2003; 34:325–337. [PubMed: 12909079]

Blaukat A, Ivankovic-Dikic I, Gronroos E, Dolfi F, Tokiwa G, Vuori K, Dikic I. Adaptor proteins Grb2 and Crk couple Pyk2 with activation of specific mitogen-activated protein kinase cascades. J Biol Chem. 1999; 274:14893–14901. [PubMed: 10329689]

Braithwaite SP, Paul S, Nairn AC, Lombroso PJ. Synaptic plasticity: one STEP at a time. Trends Neurosci. 2006; 29:452–458. [PubMed: 16806510]

Braithwaite SP, Xu J, Leung J, Urfer R, Nikolich K, Oksenberg D, Lombroso PJ, Shamloo M. Expression and function of striatal enriched protein tyrosine phosphatase is profoundly altered in cerebral ischemia. Eur J Neurosci. 2008; 27:2444–2452. [PubMed: 18445231]

Cao J, Viholainen JI, Dart C, Warwick HK, Leyland ML, Courtney MJ. The PSD95-nNOS interface: a target for inhibition of excitotoxic p38 stress-activated protein kinase activation and cell death. J Cell Biol. 2005; 168:117–126. [PubMed: 15631993]

Cowan CM, Fan MM, Fan J, Shehadeh J, Zhang LY, Graham RK, Hayden MR, Raymond LA. Polyglutamine-modulated striatal calpain activity in YAC transgenic huntington disease mouse model: impact on NMDA receptor function and toxicity. J Neurosci. 2008; 28:12725–12735. [PubMed: 19036965]

Dau A, Gladding CM, Sepers MD, Raymond LA. Chronic blockade of extrasynaptic NMDA receptors ameliorates synaptic dysfunction and pro-death signaling in Huntington disease transgenic mice. Neurobiol Dis. 2014; 62:533–542. [PubMed: 24269729]

Dunah AW, Sirianni AC, Fienberg AA, Bastia E, Schwarzschild MA, Standaert DG. Dopamine D1-dependent trafficking of striatal N-methyl-D-aspartate glutamate receptors requires Fyn protein tyrosine kinase but not DARPP-32. Mol Pharmacol. 2004; 65:121–129. [PubMed: 14722243]

Fan J, Cowan CM, Zhang LY, Hayden MR, Raymond LA. Interaction of postsynaptic density protein-95 with NMDA receptors influences excitotoxicity in the yeast artificial chromosome mouse model of Huntington's disease. J Neurosci. 2009; 29:10928–10938. [PubMed: 19726651]

Fan J, Gladding CM, Wang L, Zhang LY, Kaufman AM, Milnerwood AJ, Raymond LA. P38 MAPK is involved in enhanced NMDA receptor-dependent excitotoxicity in YAC transgenic mouse model of Huntington disease. Neurobiol Dis. 2012; 45:999–1009. [PubMed: 22198502]

Fan MM, Fernandes HB, Zhang LY, Hayden MR, Raymond LA. Altered NMDA receptor trafficking in a yeast artificial chromosome transgenic mouse model of Huntington's disease. J Neurosci. 2007; 27:3768–3779. [PubMed: 17409241]

Gafni J, Ellerby LM. Calpain activation in Huntington's disease. J Neurosci. 2002; 22:4842–4849. [PubMed: 12077181]

Ghatan S, Larner S, Kinoshita Y, Hetman M, Patel L, Xia Z, Youle RJ, Morrison RS. p38 MAP kinase mediates bax translocation in nitric oxide-induced apoptosis in neurons. J Cell Biol. 2000; 150:335–347. [PubMed: 10908576]

Gladding CM, Raymond LA. Mechanisms underlying NMDA receptor synaptic/extrasynaptic distribution and function. Mol Cell Neurosci. 2011; 48:308–320. [PubMed: 21600287]

Gladding CM, Sepers MD, Xu J, Zhang LY, Milnerwood AJ, Lombroso PJ, Raymond LA. Calpain and STriatal-Enriched protein tyrosine phosphatase (STEP) activation contribute to extrasynaptic NMDA receptor localization in a Huntington's disease mouse model. Hum Mol Genet. 2012; 21:3739–3752. [PubMed: 22523092]

Goebel-Goody SM, Davies KD, Alvestad Linger RM, Freund RK, Browning MD. Phospho-regulation of synaptic and extrasynaptic N-methyl-d-aspartate receptors in adult hippocampal slices. Neuroscience. 2009; 158:1446–1459. [PubMed: 19041929]

Gomez-Lazaro M, Galindo MF, Melero-Fernandez de Mera RM, Fernandez-Gomez FJ, Concannon CG, Segura MF, Comella JX, Prehn JH, Jordan J. Reactive oxygen species and p38 mitogen-activated protein kinase activate Bax to induce mitochondrial cytochrome c release and apoptosis in response to malonate. Mol Pharmacol. 2007; 71:736–743. [PubMed: 17172466]

Graham RK, Pouladi MA, Joshi P, et al. Differential susceptibility to excitotoxic stress in YAC128 mouse models of Huntington disease between initiation and progression of disease. J Neurosci. 2009; 29:2193–2204. [PubMed: 19228972]

Hardingham GE, Fukunaga Y, Bading H. Extrasynaptic NMDARs oppose synaptic NMDARs by triggering CREB shut-off and cell death pathways. Nat Neurosci. 2002; 5:405–414. [PubMed: 11953750]

HDCRG. A novel gene containing a trinucleotide repeat that is expanded and unstable on Huntington's disease chromosomes. The Huntington's Disease Collaborative Research Group. Cell. 1993; 72:971–983. [PubMed: 8458085]

Jiang X, Knox R, Pathipati P, Ferriero D. Developmental localization of NMDA receptors, Src and MAP kinases in mouse brain. Neurosci Lett. 2011; 503:215–219. [PubMed: 21896318]

Johnson MA, Lombroso PJ. A common STEP in the synaptic pathology of diverse neuropsychiatric disorders. Yale J Biol Med. 2012; 85:481–490. [PubMed: 23239949]

Kim YJ, Yi Y, Sapp E, Wang Y, Cuiffo B, Kegel KB, Qin ZH, Aronin N, DiFiglia M. Caspase 3-cleaved N-terminal fragments of wild-type and mutant huntingtin are present in normal and Huntington's disease brains, associate with membranes, and undergo calpain-dependent proteolysis. Proc Natl Acad Sci U S A. 2001; 98:12784–12789. [PubMed: 11675509]

Lau CG, Zukin RS. NMDA receptor trafficking in synaptic plasticity and neuropsychiatric disorders. Nat Rev Neurosci. 2007; 8:413–426. [PubMed: 17514195]

Lev S, Moreno H, Martinez R, Canoll P, Peles E, Musacchio JM, Plowman GD, Rudy B, Schlessinger J. Protein tyrosine kinase PYK2 involved in Ca(2+)-induced regulation of ion channel and MAP kinase functions. Nature. 1995; 376:737–745. [PubMed: 7544443]

Leveille F, El Gaamouch F, Gouix E, Lecocq M, Lobner D, Nicole O, Buisson A. Neuronal viability is controlled by a functional relation between synaptic and extrasynaptic NMDA receptors. Faseb J. 2008; 22:4258–4271. [PubMed: 18711223]

Li L, Murphy TH, Hayden MR, Raymond LA. Enhanced striatal NR2B-containing N-methyl-D-aspartate receptor-mediated synaptic currents in a mouse model of Huntington disease. J Neurophysiol. 2004; 92:2738–2746. [PubMed: 15240759]

Liu YF, Dorow D, Marshall J. Activation of MLK2-mediated signaling cascades by polyglutamine-expanded huntingtin. J Biol Chem. 2000; 275:19035–19040. [PubMed: 10801775]

Milnerwood AJ, Gladding CM, Pouladi MA, et al. Early increase in extrasynaptic NMDA receptor signaling and expression contributes to phenotype onset in Huntington's disease mice. Neuron. 2010; 65:178–190. [PubMed: 20152125]

Nguyen TH, Liu J, Lombroso PJ. Striatal enriched phosphatase 61 dephosphorylates Fyn at phosphotyrosine 420. J Biol Chem. 2002; 277:24274–24279. [PubMed: 11983687]

Pacchioni AM, Vallone J, Worley PF, Kalivas PW. Neuronal pentraxins modulate cocaine-induced neuroadaptations. J Pharmacol Exp Ther. 2009; 328:183–192. [PubMed: 18840757]

Paul S, Nairn AC, Wang P, Lombroso PJ. NMDA-mediated activation of the tyrosine phosphatase STEP regulates the duration of ERK signaling. Nat Neurosci. 2003; 6:34–42. [PubMed: 12483215]

Paul S, Snyder GL, Yokakura H, Picciotto MR, Nairn AC, Lombroso PJ. The Dopamine/D1 receptor mediates the phosphorylation and inactivation of the protein tyrosine phosphatase STEP via a PKA-dependent pathway. J Neurosci. 2000; 20:5630–5638. [PubMed: 10908600]

Poddar R, Deb I, Mukherjee S, Paul S. NR2B-NMDA receptor mediated modulation of the tyrosine phosphatase STEP regulates glutamate induced neuronal cell death. J Neurochem. 2010; 115:1350–1362. [PubMed: 21029094]

Rumbaugh G, Adams JP, Kim JH, Huganir RL. SynGAP regulates synaptic strength and mitogen-activated protein kinases in cultured neurons. Proc Natl Acad Sci U S A. 2006; 103:4344–4351. [PubMed: 16537406]

Saavedra A, Giralt A, Rue L, et al. Striatal-enriched protein tyrosine phosphatase expression and activity in Huntington's disease: a STEP in the resistance to excitotoxicity. J Neurosci. 2011; 31:8150–8162. [PubMed: 21632937]

Shehadeh J, Fernandes HB, Zeron Mullins MM, Graham RK, Leavitt BR, Hayden MR, Raymond LA. Striatal neuronal apoptosis is preferentially enhanced by NMDA receptor activation in YAC transgenic mouse model of Huntington disease. Neurobiol Dis. 2006; 21:392–403. [PubMed: 16165367]

Soriano FX, Martel MA, Papadia S, et al. Specific targeting of pro-death NMDA receptor signals with differing reliance on the NR2B PDZ ligand. J Neurosci. 2008; 28:10696–10710. [PubMed: 18923045]

Xu J, Kurup P, Bartos JA, Patriarchi T, Hell JW, Lombroso PJ. Striatal-enriched protein-tyrosine phosphatase (STEP) regulates Pyk2 kinase activity. J Biol Chem. 2012; 287:20942–20956. [PubMed: 22544749]

Xu J, Kurup P, Zhang Y, Goebel-Goody SM, Wu PH, Hawasli AH, Baum ML, Bibb JA, Lombroso PJ. Extrasynaptic NMDA receptors couple preferentially to excitotoxicity via calpain-mediated cleavage of STEP. J Neurosci. 2009; 29:9330–9343. [PubMed: 19625523]

Zeron MM, Hansson O, Chen N, Wellington CL, Leavitt BR, Brundin P, Hayden MR, Raymond LA. Increased sensitivity to N-methyl-D-aspartate receptor-mediated excitotoxicity in a mouse model of Huntington's disease. Neuron. 2002; 33:849–860. [PubMed: 11906693]

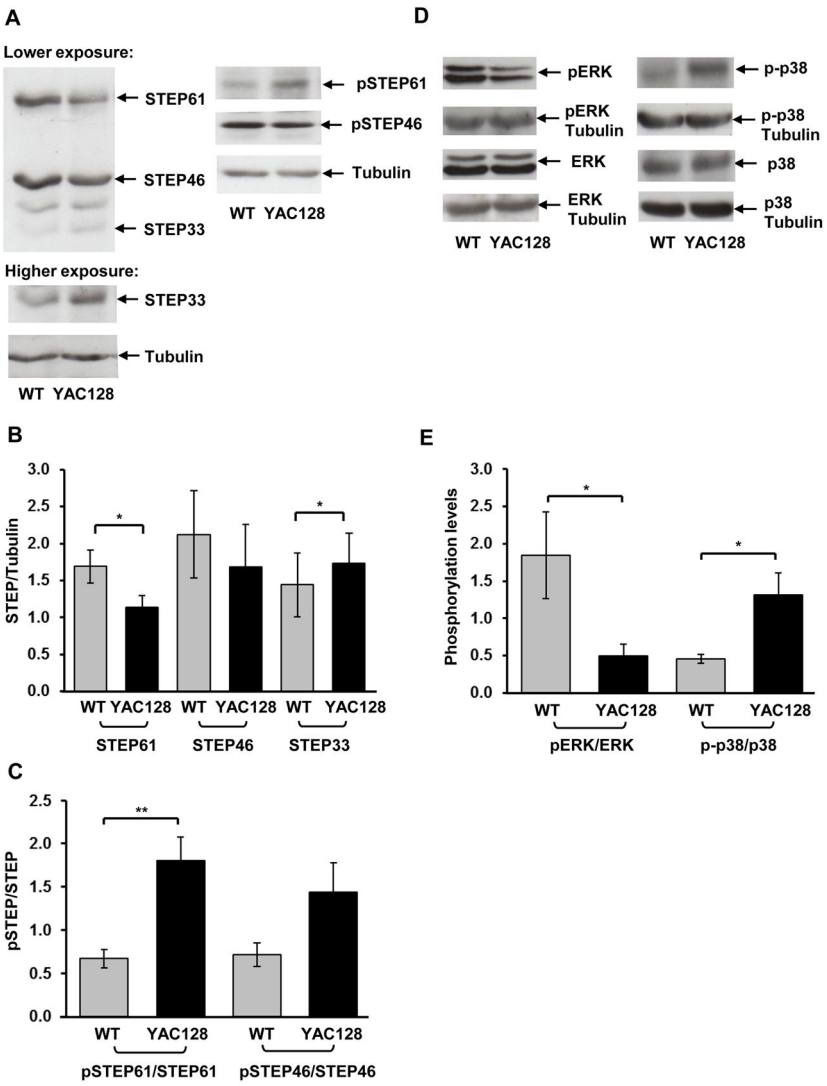

Figure 1.

In 6-week old, excitotoxin-sensitive YAC128 mice, elevated STEP61 cleavage is associated with increased STEP61 phosphorylation, decreased ERK1/2 phosphorylation and increased p38 phosphorylation levels. **A)** Representative immunoblots of WT and YAC128 striatal whole-cell lysates probed for STEP, pSTEP and tubulin. Lower exposure blots were used for all quantification apart for STEP33 where the higher exposure was used. **B)** Quantification of STEP61/tubulin, STEP46/tubulin and STEP33/tubulin ratios. **C)** Quantification of pSTEP61/STEP61 and pSTEP46/STEP46 ratios. YAC128 mice show significantly reduced STEP61 levels and significantly increased STEP33 levels. STEP61 phosphorylation is also significantly increased in YAC128 mice compared to WT. Significance tested using twotailed paired *t*-tests (*$p < 0.05$, **$p < 0.01$, n = 6–8). **D)** Representative immunoblots of WT and YAC128 striatal whole-cell lysates probed with ERK, phosphorylated ERK (pERK), p38, phosphorylated p38 (p-p38) and tubulin antibodies. **E)** Quantification of p-ERK/ERK and p-p38/p38 MAPK ratios after normalization to tubulin. In the presymptomatic YAC128 striatum, ERK1/2 phosphorylation is significantly decreased

whereas p38 MAPK phosphorylation is significantly increased relative to WT mice. Significance tested using two-tailed paired *t*-tests (*$p < 0.05$, n = 7–8).

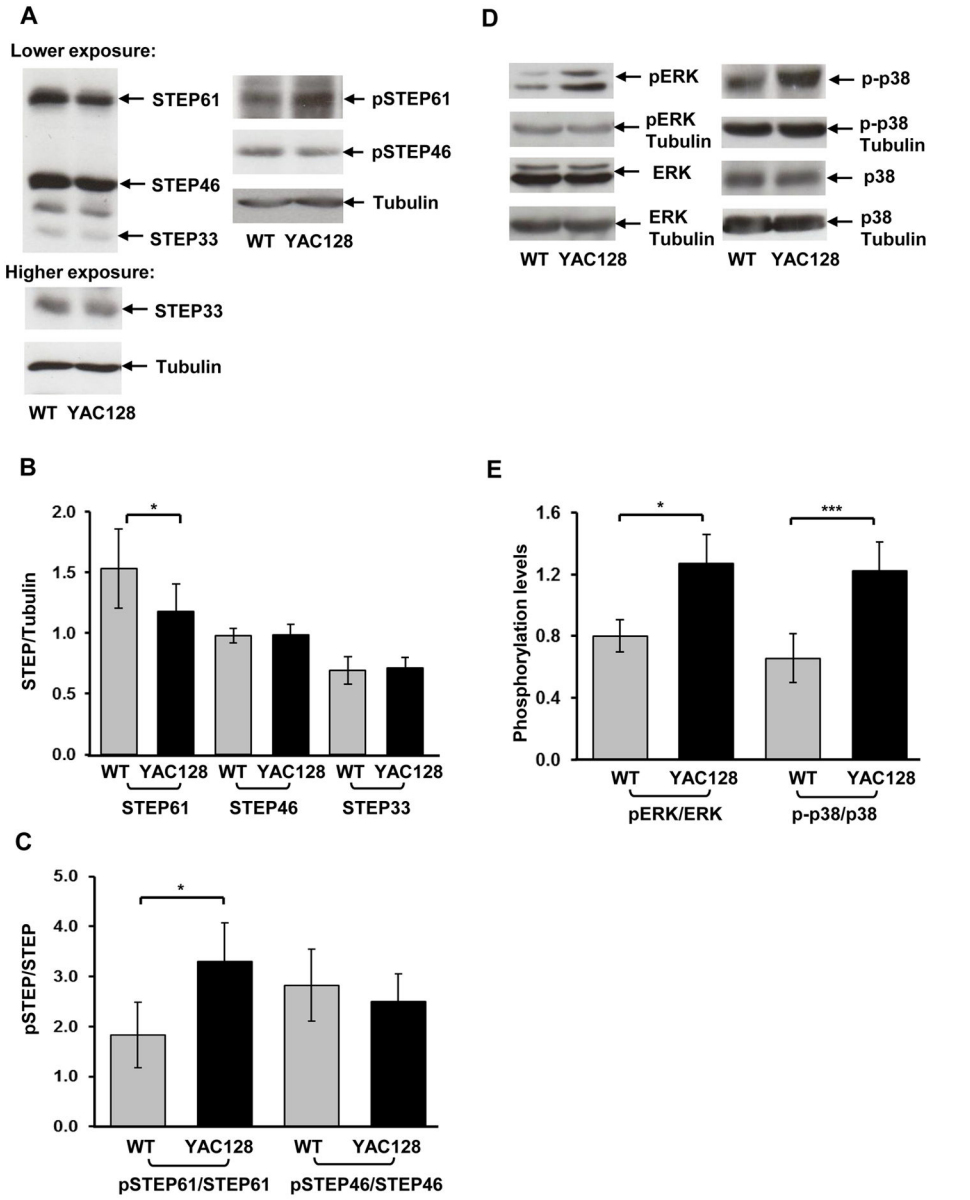

Figure 2.

The striatum of 1-year old, excitotoxin-resistant YAC128 mice shows decreased STEP61 levels, elevated STEP61 phosphorylation as well as increased ERK1/2 and p38 MAPK phosphorylation. **A)** Representative immunoblots of striatal whole-cell lysates isolated from 1-year old WT and YAC128 mice, probed for STEP, pSTEP and tubulin. Lower exposure blots were used for all quantification apart for STEP33 where the higher exposure was used. **B)** Quantification of STEP61/tubulin, STEP46/tubulin and STEP33/tubulin ratios. **C)** Quantification of pSTEP61/STEP61 and pSTEP46/STEP46 ratios. YAC128 mice have significantly reduced STEP61 levels and significantly increased STEP61 phosphorylation compared to WT mice. Significance tested using two-tailed paired *t*-tests (*$p < 0.05$, n = 8). **D)** Representative immunoblots of WT and YAC128 striatal whole-cell lysates probed with ERK, pERK, p38, p-p38 and tubulin antibodies. **E)** Quantification of p-ERK/ERK and p-

p38/p38 MAPK ratios after normalization to tubulin. In the striatum from 1-year old YAC128 mice, ERK1/2 and p38 MAPK phosphorylation levels are both significantly increased relative to WT mice. Significance tested using two-tailed paired *t*-tests (*$p < 0.05$, ***$p < 0.001$, n = 8).

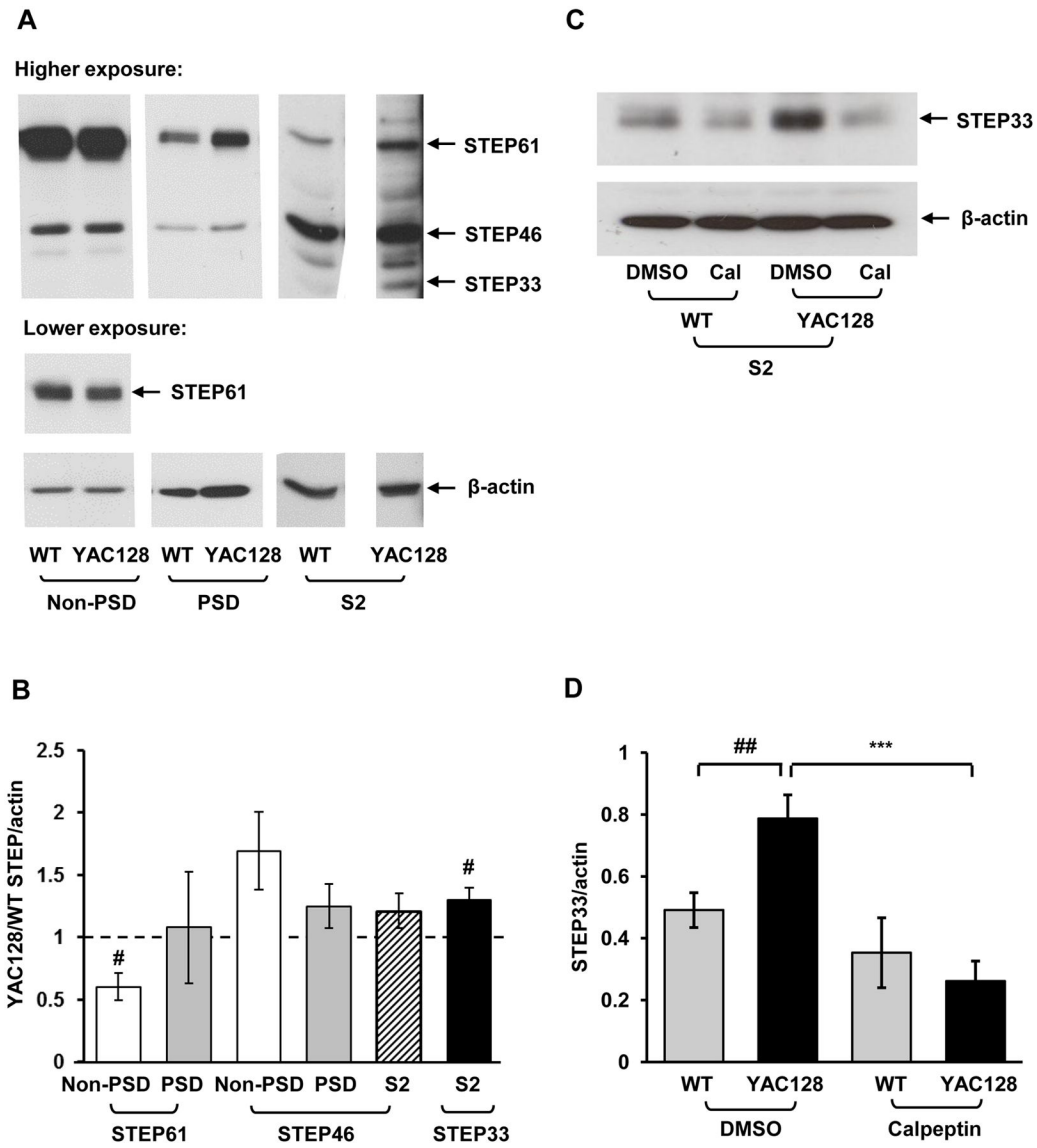

Figure 3.

In 6-week old presymptomatic YAC128 mice, extrasynaptic calpain cleavage of STEP61 is increased in the striatum but decreased by calpeptin treatment. **A)** Representative immunoblots of WT and YAC128 striatal non-PSD, PSD and S2 (cytosolic) fractions probed for STEP and β-actin. Higher exposure blots were used for all quantification apart for STEP61 in the non-PSD where the lower exposure was used. **B)** Quantification of non-PSD and PSD STEP61 and STEP46/β-actin ratios and cytosolic STEP46 and STEP33/β-actin ratios in YAC128 mice relative to WT. YAC128 mice have significantly reduced non-PSD STEP61 levels and significantly increased cytosolic STEP33 levels. Significance tested using one-sample *t*-tests (#$p < 0.05$, n = 7). **C)** Representative immunoblots of WT and YAC128 striatal cytosolic fractions isolated from parasagittal slices treated with either DMSO (vehicle) or calpeptin (Cal, 15μM, 2h), and probed with STEP and β-actin antibodies. **D)** Quantification of DMSO- and calpeptin-treated STEP33/β-actin ratios.

Calpain inhibition significantly reduces YAC128 STEP33 levels, which were significantly higher than WT in the DMSO-treated condition. An unpaired *t*-test revealed a significant difference between WT and YAC128 STEP33/β-actin ratios in the vehicle (DMSO treatment) condition (##$p < 0.01$). A two-way ANOVA indicated significant differences for treatment ($F_{1,12} = 27.58$, ***$p < 0.001$) and interaction ($F_{1,12} = 9.41$, **$p < 0.01$); ***$p < 0.001$ by Bonferroni *post hoc* test; n = 7.

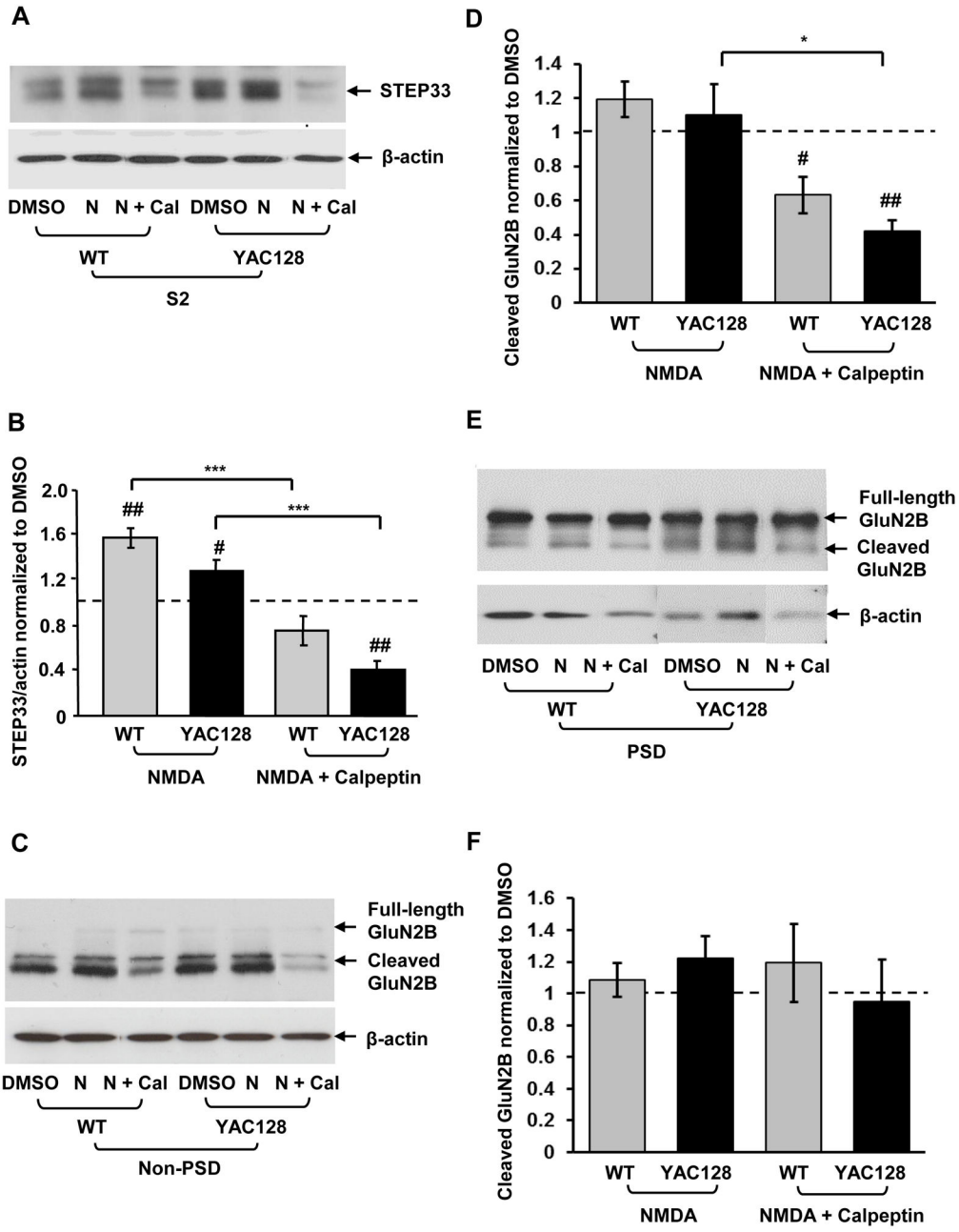

Figure 4.

Calpain inhibition decreases NMDA-induced calpain cleavage of STEP61 and GluN2B in 6-week old excitotoxin-sensitive YAC128 mice. **A)** Representative immunoblots of striatal S2 (cytosolic) fractions isolated from WT and YAC128 striatal tissue from parasagittal slices treated with either DMSO (vehicle) or NMDA (N; 30μM, 70min) with or without calpeptin (Cal, 15μM). Samples were probed for STEP and β-actin. **B)** Quantification of cytosolic STEP33/β-actin ratios after treatment with NMDA alone or NMDA with calpeptin, normalized to DMSO. One-sample *t*-tests revealed significant increases in WT and YAC128 STEP33 levels after NMDA treatment relative to the vehicle control (##$p < 0.01$; #$p < 0.05$).

Calpeptin significantly reduces NMDA-induced STEP33 production in the striatum from both 6-week old WT and YAC128 mice. Significant differences were detected for treatment ($F_{1,8} = 91.73$, ***$p < 0.001$) and genotype ($F_{1,8} = 9.69$, *$p < 0.05$) with a two-way ANOVA; ***$p < 0.001$ by Bonferroni *post hoc* test; n = 5. **C)** Representative immunoblots of WT and YAC128 striatal non-PSD fractions probed with N-terminal GluN2B and β-actin antibodies. **D)** Quantification of non-PSD cleaved GluN2B/β-actin ratios normalized to DMSO (vehicle) after NMDA treatment with or without calpeptin. With NMDA, calpain inhibition significantly reduces cleaved GluN2B levels in the YAC128 but not WT striatum. Relative to basal (DMSO-treated) levels, significant differences in cleaved GluN2B were detected with one-sample *t*-tests (##$p < 0.01$; #$p < 0.05$). Significance was also detected using a two-way ANOVA for treatment ($F_{1,6} = 20.48$, **$p < 0.01$); *$p < 0.05$ by Bonferroni *post hoc* test; n = 4. **E)** Representative immunoblots of WT and YAC128 striatal PSD fractions probed for GluN2B and β-actin. **F)** The effect of NMDA with or without calpeptin on synaptic cleaved GluN2B levels was quantified relative to DMSO. There was no effect of NMDA or calpeptin on synaptic GluN2B levels (tested using a two-way ANOVA, $p > 0.05$; n = 5).

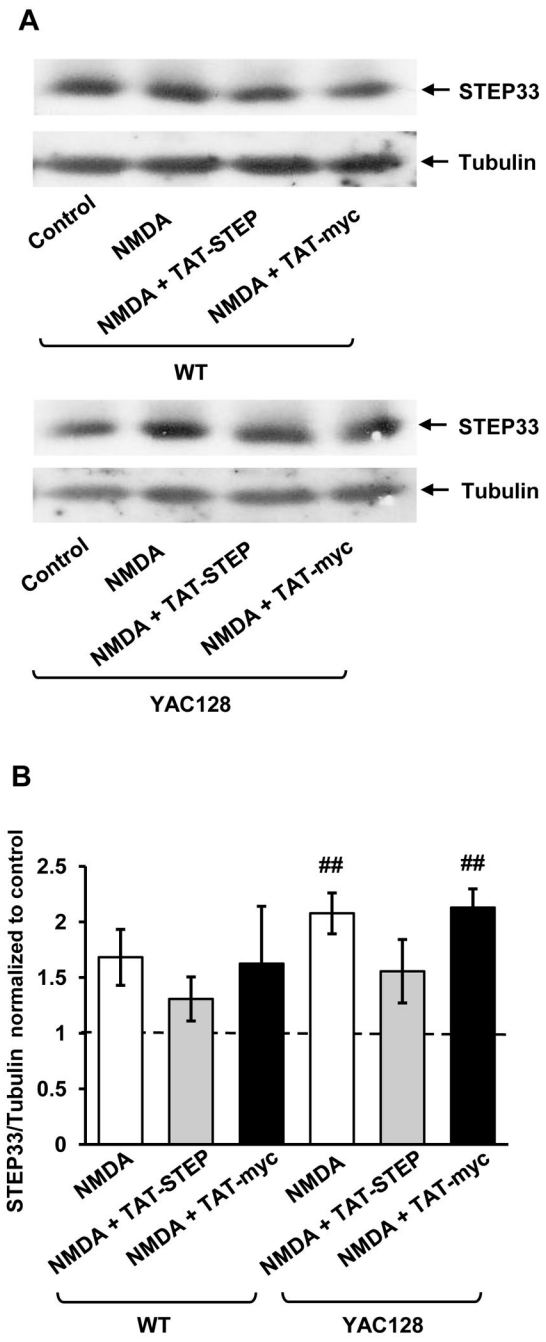

Figure 5.

Specific inhibition of NMDA-induced calpain cleavage of STEP61 in the striatum of 6-week old YAC128 mice. **A)** Representative immunoblots of striatal whole-cell lysates obtained from WT and YAC128 parasagittal slices untreated (control) or treated with NMDA (30μM, 70min) with either the TAT-STEP calpain cleavage inhibitory peptide (2μM, 70min) or the TAT-myc (control) peptide (2μM, 70min). Samples were probed for STEP and the loading control tubulin. **B)** Quantification of STEP33/tubulin ratios after NMDA with or without peptide, normalized to the control untreated condition. NMDA significantly increases

STEP33 levels in 6-week old YAC128 but not WT striatum but not in the presence of the TAT-STEP calpain cleavage inhibitory peptide. Statistics performed using one-sample *t*-tests (##$p < 0.01$, n = 4).

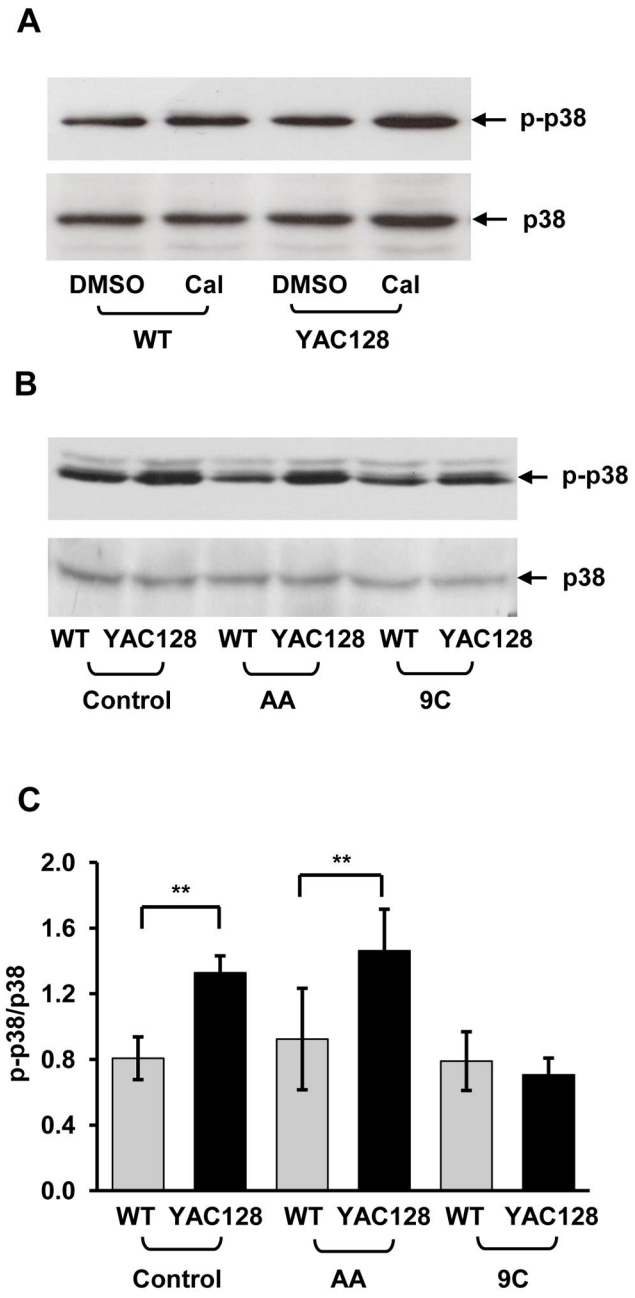

Figure 6.

GluN2B-PSD-95 binding rather than calpain-mediated cleavage of STEP contributes to increased basal p38 MAPK activation in 6-week old presymptomatic YAC128 mice. **A)** Representative immunoblots of striatal cytosolic fractions obtained from WT and YAC128 parasagittal slices treated with either DMSO (vehicle) or calpeptin (Cal, 15μM, 2h). Samples were probed with either p38 or p-p38 antibodies. Calpeptin had no effect on p-p38/p38 ratios in either WT or YAC128 striatum (quantification not shown). **B)** Representative immunoblots of striatal whole-cell lysates obtained from WT and YAC128 parasagittal slices treated with either the TAT-GluN2B9c peptide or control TAT-GluN2BAA peptide (200nM, 1h). Samples were probed with either p-p38 or p38 MAPK antibodies. **C)**

Quantification of p-p38/p38 density ratios after TAT-GluN2B9C or AA peptide treatment. The TAT-GluN2B9c but not the AA peptide significantly reduces basal p38 activation in the striatum from 6-week old YAC128 but not WT mice. A two-way ANOVA revealed significant differences for genotype ($F_{1,12} = 20.60$, ***$p < 0.001$), interaction ($F_{2,12} = 6.96$, **$p < 0.01$) and subjects (matching) ($F_{12,12} = 8.89$, ***$p < 0.001$); **$p < 0.01$ by Bonferroni *post hoc* test; n = 5.